

# **Mn carbonyl complexes as selective electrocatalysts for CO<sub>2</sub> reduction in water and organic solvents**

Bhavin Siritanaratkul, Catherine Eagle and Alexander J. Cowan\*

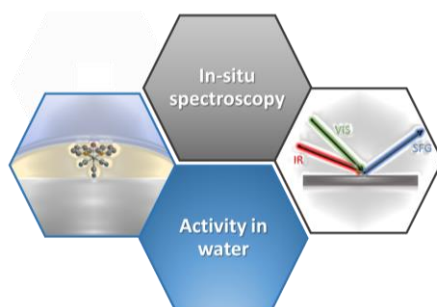
Stephenson Institute for Renewable Energy and the Department of Chemistry

University of Liverpool

Liverpool, L69 7ZF, UK

\*acowan@liverpool.ac.uk

## Conspectus



The electrochemical reduction of CO<sub>2</sub> provides a way to sustainably generate carbon-based fuels and feedstocks. Molecular CO<sub>2</sub> reduction electrocatalysts provide tuneable reaction centres offering an approach to control the selectivity of catalysis. Mn carbonyl complexes, based on [Mn(bpy)(CO)<sub>3</sub>Br] and its derivatives (bpy = 2, 2'-bipyridine) are particularly interesting due to their ease of synthesis and the use of a first-row earth-abundant transition metal. [Mn(bpy)(CO)<sub>3</sub>Br] was first shown to be an active and selective catalyst for reducing CO<sub>2</sub> to CO in organic solvents in 2011. Since then, Mn carbonyl catalysts have been widely studied with numerous reports of their use as electrocatalysts, photocatalysts and studies of their mechanism.

This class of Mn catalysts only shows CO<sub>2</sub> reduction activity with the addition of weak Brønsted acids. Perhaps surprisingly, early reports showed increased turnover frequencies as the acid strength is increased without a loss in selectivity towards CO evolution. It may have been expected that competing hydrogen evolution reaction could have led to lower selectivity. Inspired by these works we began to explore if the catalyst would work in protic solvents, namely water and to explore the pH range over which it can operate. Here we describe the early studies from our laboratory that first demonstrated the use of Mn carbonyl complexes as CO<sub>2</sub> reduction electrocatalysts in water and then go on to discuss wider developments on the use of these catalysts in water, highlighting their potential as catalysts for use in aqueous CO<sub>2</sub> electrolyzers.

Key to the excellent selectivity of these catalysts in the presence of Brønsted acids is a proton assisted CO<sub>2</sub> binding mechanism, where for the acids widely studied, lower pK<sub>a</sub>'s actually favour CO<sub>2</sub> binding over Mn-H formation, a precursor to H<sub>2</sub> evolution. Here we discuss the wider literature before focusing on our own contributions in validating this previously proposed mechanism through the use of vibrational sum frequency generation (VSFG) spectroelectrochemistry. This allowed us to study [Mn(bpy)(CO)<sub>3</sub>Br] whilst it is at, or near, the electrode surface which provided a way to identify new catalytic intermediates and also confirm that proton assisted CO<sub>2</sub> binding operates in both the "dimer" and primary (via [Mn(bpy)(CO)<sub>3</sub>]<sup>-</sup>) pathways. Understanding the mechanism of how these highly

selective catalysts operate is important as we propose that the Mn complexes will be valuable models to guide the development of new proton/acid tolerant CO<sub>2</sub> reduction catalysts.

## Key references

- Walsh, J. J.; Neri, G.; Smith, C. L.; Cowan, A. J., Electrocatalytic CO<sub>2</sub> reduction with a membrane supported manganese catalyst in aqueous solution. *Chem. Commun.* **2014**, 50 (84), 12698-12701.<sup>1</sup> *This paper used a simple approach to immobilise the Mn complex on a carbon support allowing for its study in aqueous solvent for the first time, demonstrating that CO<sub>2</sub> reduction selectivity was retained.*
- Walsh, J. J.; Neri, G.; Smith, C. L.; Cowan, A. J., Water-Soluble Manganese Complex for Selective Electrocatalytic CO<sub>2</sub> Reduction to CO. *Organometallics* **2019**, 38 (6), 1224-1229.<sup>2</sup> *Here we showed the activity and selectivity of a carboxylic acid derivative in water across a wide pH range.*
- Neri, G.; Walsh, J. J.; Teobaldi, G.; Donaldson, P. M.; Cowan, A. J., Detection of catalytic intermediates at an electrode surface during carbon dioxide reduction by an earth-abundant catalyst. *Nature Catalysis* **2018**, 1 (12), 952-959.<sup>3</sup> *This study used vibrational sum-frequency generation spectroscopy to follow the reaction mechanisms of the Mn catalyst transiently at an electrode during carbon dioxide reduction.*
- Neri, G.; Donaldson, P. M.; Cowan, A. J., In situ study of the low overpotential “dimer pathway” for electrocatalytic carbon dioxide reduction by manganese carbonyl complexes. *Physical Chemistry Chemical Physics* **2019**, 21 (14), 7389-7397.<sup>4</sup> *Here we examined the surface behaviour of the Mn catalyst as it arrives at the electrode and also explored the mechanism of the less studied lower overpotential reaction pathway.*

## 1. Introduction

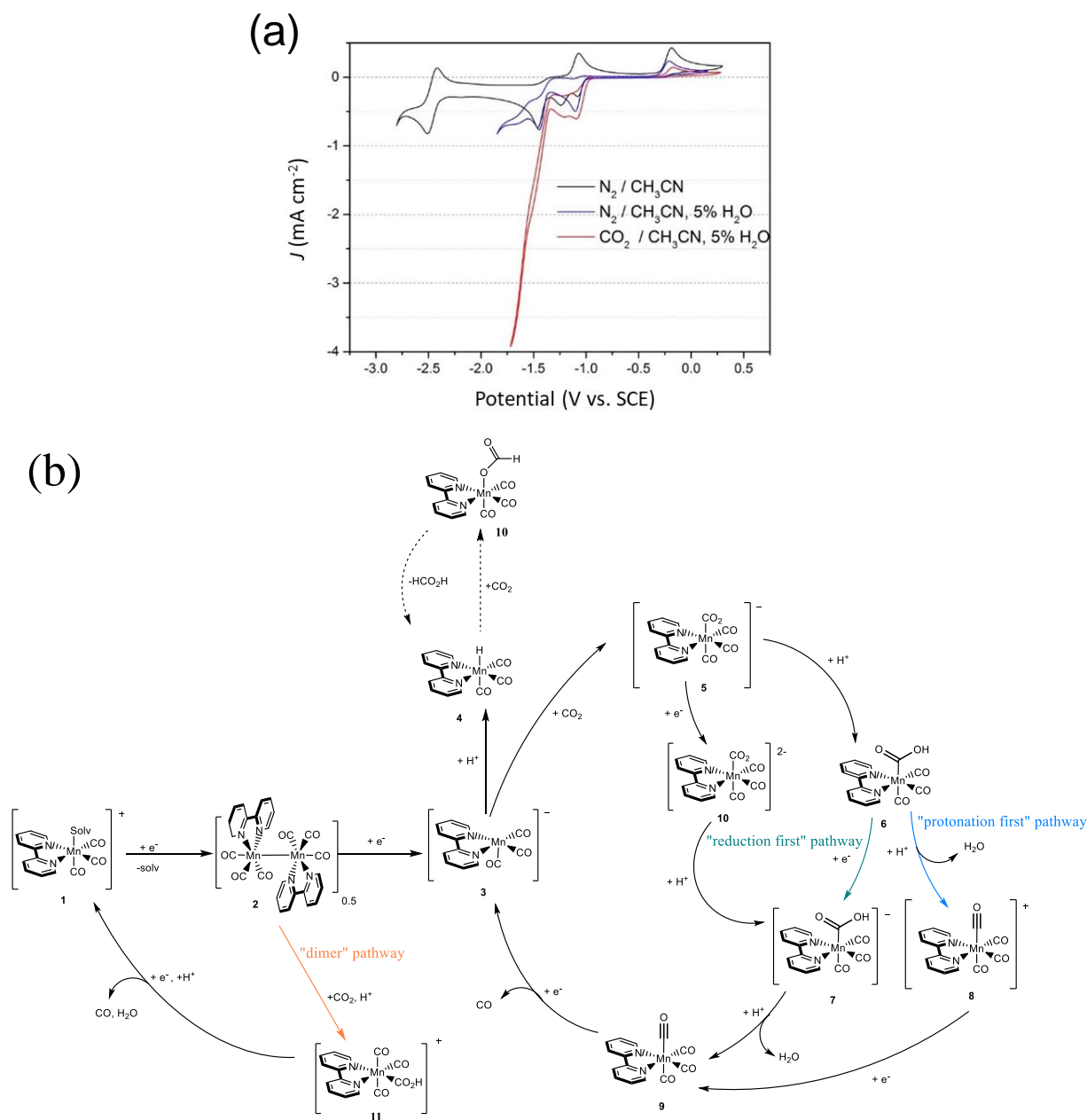
Electrochemical CO<sub>2</sub> reduction will be needed to enable a circular carbon economy and it is proposed to play an important role in managing CO<sub>2</sub> emissions.<sup>5-7</sup> Electrochemical CO<sub>2</sub> conversion at scale is expected to make use of point sources of CO<sub>2</sub>, such as flue gas from heavy industries. Metal electrodes and metallic electrocatalysts<sup>8</sup> deposited onto high surface area supports have demonstrated that reduction of pure CO<sub>2</sub> feeds can achieve high current densities (up to 1 A cm<sup>-2</sup>) in CO<sub>2</sub> electrolyzers.<sup>9</sup> However, as the CO<sub>2</sub> concentration is decreased and impurities such as, O<sub>2</sub>, NO<sub>x</sub> and SO<sub>x</sub>, are added to simulate a typical flue gas stream, changes in selectivity have been reported.<sup>10, 11</sup> Molecular catalysts<sup>12-15</sup> provide an opportunity to achieve desired reactant and product selectivity by altering the ligands surrounding the metal centre to tune the reaction centre’s electronics and steric bulk. Therefore, they are particularly interesting as both models of how CO<sub>2</sub> selectivity can be controlled, and as potential practical-scale catalysts for application in an immobilized configuration.

A widely studied class of molecular electrocatalysts is those based on [*fac*- Re(bpy)(CO)<sub>3</sub>Cl] (bpy = 2,2'-bipyridine, hereafter the *fac*- is assumed for all tricarbonyl structures unless otherwise stated). This catalyst was first reported in the 1980s to produce CO both photocatalytically and electrochemically from CO<sub>2</sub>, displaying high Faradaic efficiencies for CO and a good stability under electrocatalytic conditions.<sup>16,17</sup> Despite these promising results, Re has a low natural abundance.<sup>18</sup> Early on, [Mn(bpy)(CO)<sub>3</sub>Br] was examined as a possible alternative high-abundance catalyst, but initial reports in organic solvents noted a lack of activity towards CO<sub>2</sub>.<sup>19</sup> It was not until 2011 in a breakthrough study by Deronzier and co-workers<sup>20</sup> that [Mn(bpy-R)(CO)<sub>3</sub>Br] (R = H or alkyl group at the 4,4' position) was shown to be an active electrocatalyst for CO<sub>2</sub> reduction in organic solvents, but only when a Brønsted acid was added. A typical cyclic voltammogram of [Mn(bpy)(CO)<sub>3</sub>Br] in acetonitrile, similar to that measured in those first reports, is shown in Figure 1a, and a proposed catalytic cycle is shown in Figure 1b. Under N<sub>2</sub>, initial reduction at -1.2 V<sub>SCE</sub> results in the loss of Br<sup>-</sup> and then dimerization to form [Mn(bpy)(CO)<sub>3</sub>]<sub>2</sub>. This dimer complex is reduced at -1.5 V<sub>SCE</sub> to form the main catalytically active species [Mn(bpy)(CO)<sub>3</sub>]<sup>-</sup> as indicated by the large increase in current under CO<sub>2</sub> and in the presence of a proton source. In competition with CO evolution is H<sub>2</sub> production which occurs via the formation of [Mn(bpy)(CO)<sub>3</sub>H].

The initial study by Deronzier and colleagues<sup>20</sup> led to a large number of follow-on works on this class of catalyst, of which several reviews exist.<sup>13,21-24</sup> In this Account we discuss one of the most interesting aspects, the need for a Brønsted acid for any measurable CO<sub>2</sub> reduction to occur.<sup>16,17</sup> This finding was confirmed in a study by the Kubiak group in 2013, on a derivative, [Mn(bpy(<sup>t</sup>Bu)<sub>2</sub>)(CO)<sub>3</sub>Br], in acetonitrile with the addition of the weak acids: water, methanol and 2,2,2-trifluoroethanol (TFE), where higher turnover frequencies were achieved than with the parent complex.<sup>25</sup> Also, the turnover frequency of the Mn catalyst was shown to increase with acid strength, and in general with higher concentrations of acid, without a loss in selectivity towards CO<sub>2</sub> reduction. These experiments on the complex in aprotic solvents with an acid source led us to ask in 2014;<sup>1</sup> could the performance of [Mn(bpy)(CO)<sub>3</sub>Br] be further improved by use in a protic solvent, in particular water?

Developing CO<sub>2</sub> reduction catalysts that are selective in water is important; in a practical electrolyser the CO<sub>2</sub> reduction reaction will need to be coupled to a sustainable oxidation reaction, presumably water oxidation. In particular there is current interest in understanding how to develop systems that can selectively reduce CO<sub>2</sub> in an acidic environment<sup>26</sup> as operating CO<sub>2</sub> electrolysers at high pH's leads to carbonate formation with consequential decreased CO<sub>2</sub> conversion efficiencies.<sup>27</sup> With conventional metal catalysts (e.g. Ag, Au, Cu) operating at low pH is challenging due to competitive hydrogen evolution as a result of the high proton concentration. Therefore, the development and mechanistic study of molecular electrocatalysts that show a high selectivity to CO<sub>2</sub> reduction in the presence of high proton concentrations is of great interest to the field. Here we describe in Section 2 the

use of this class of Mn catalysts for CO<sub>2</sub> reduction in water, focusing on early work from our own laboratory before discussing wider developments in the field. In Section 3 we discuss mechanistic studies on the role of the acid source in the CO<sub>2</sub> reduction mechanism in an effort to understand how these catalysts achieve selectivity. In particular we introduce the use of VSFG spectroscopy which confirmed a previously proposed proton-assisted CO<sub>2</sub> binding mechanism for the main catalytic pathways, rationalizing why these catalysts can operate even in proton-rich environments.



studies.<sup>22</sup> These are the dimer pathway (orange), protonation first pathway (blue) and reduction first pathway (green). An additional proposed pathway to form formate/formic acid is also shown<sup>28</sup> (dashed lines). Figure 1(b) is adapted from reference<sup>3</sup> with permission from Springer Nature.

## 2. [Mn(bpy)(CO)<sub>3</sub>Br] and its derivatives as CO<sub>2</sub> reduction catalysts in water

To test how [Mn(bpy)(CO)<sub>3</sub>Br] behaved in the presence of aqueous electrolytes we initially applied a simple approach previously described for a range of catalysts including [Re(bpy)(CO)<sub>3</sub>Br],<sup>29</sup> where we deposited the Mn complex directly onto a glassy carbon electrode (GCE) using a Nafion ionomer support.<sup>1</sup> Direct study of the mechanism of the catalyst within the Nafion membrane is challenging but CV's indicated that despite being immobilized and used at pH 7, the catalyst showed very similar behaviour to that observed when dissolved in aprotic solvents with the largest current enhancement under CO<sub>2</sub> occurring following the formation of [Mn(bpy)(CO)<sub>3</sub>]. Intriguingly in the Nafion membrane dimerization is believed to still occur following initial reduction of [Mn(bpy)(CO)<sub>3</sub>Br], prior to the formation of the active [Mn(bpy)(CO)<sub>3</sub>]<sup>-</sup> catalyst, as indicated by the oxidation peak of [Mn<sub>2</sub>(bpy)<sub>2</sub>(CO)<sub>6</sub>]. A linear dependence of peak current for the reduction of [Mn(bpy)(CO)<sub>3</sub>Br] indicated that the complex was not solubilized in the polymer and no evidence of Mn loss into the electrolyte was found suggesting that the dimer formation was the result of electroactive aggregates, however definitive evidence of the mechanism of dimerization within Nafion is still missing. Regardless of the possible mechanisms of dimerization the most important outcome of this first study however was that once formed [Mn(bpy)(CO)<sub>3</sub>]<sup>-</sup> displayed good selectivity for CO<sub>2</sub> reduction in water at pH 7 with a CO:H<sub>2</sub> ratio of 2:1 being achieved at -1.4 V<sub>Ag/AgCl</sub>, and TON of up to 470. This demonstrated the viability of using this complex in protic solvents and indicates that CO<sub>2</sub> reduction selectivities on a par with those seen in aprotic solvents could be achieved.

In the first studies of GCE/[Mn(bpy)(CO)<sub>3</sub>Br]/Nafion electrodes current densities were low (0.3 mA cm<sup>-2</sup>) due to the majority of the catalyst present being electro-inactive. The addition of multi-walled carbon nanotubes (MWCNT), increasing the electroactive content, led to a large increase in current density under CO<sub>2</sub> (up to 3 mA cm<sup>-2</sup>, Figure 2), albeit with a partial loss in CO:H<sub>2</sub> selectivity (dropping to ~1:2).<sup>1</sup> A subsequent study investigated a wider range of Mn complexes which contained modifications to the 4,4' positions of the 2,2'-bipyridine ligand immobilized in a similar manner with MWCNT.<sup>30</sup> Amongst the complexes studied [Mn(bpy(<sup>t</sup>Bu)<sub>2</sub>)(CO)<sub>3</sub>Br], which was first reported by Kubiak and colleagues,<sup>25</sup> gave the highest level of selectivity towards CO (CO:H<sub>2</sub> ~1) however the CO partial current density was lower than the original unmodified bipyridine complex. Also studied were [Mn(bpy(OH)<sub>2</sub>)(CO)<sub>3</sub>Br] and [Mn(bpy(COOH)<sub>2</sub>)(CO)<sub>3</sub>Br], but both complexes gave disappointing levels of selectivity when immobilised, with CO:H<sub>2</sub> ~ 0.28 and 0.33, respectively.<sup>30</sup> The initial studies of the Mn catalysts deposited on GCE made use of the low solubility of [Mn(bpy)(CO)<sub>3</sub>Br] in water<sup>1, 30</sup>

however relatively low electroactive contents were achieved and the current densities reported above are ~30 times lower than is required for application in a practical electrolyser ( $>100 \text{ mA cm}^{-2}$ ).

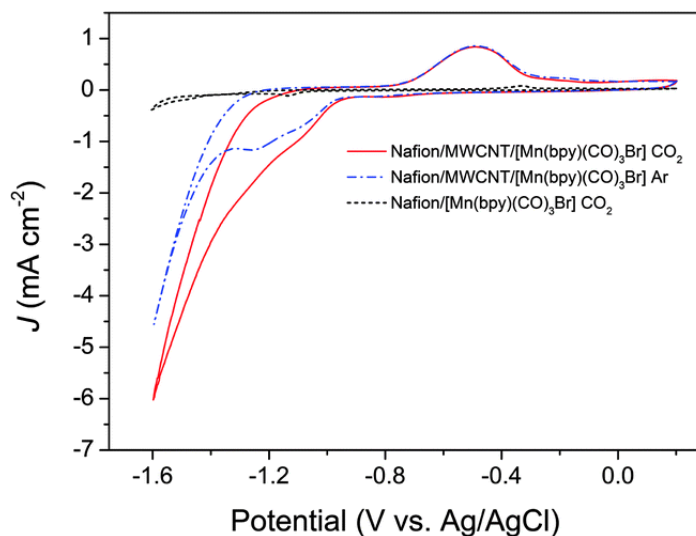


Figure 2. Cyclic voltammetry of  $[\text{Mn}(\text{bpy})(\text{CO})_3\text{Br}]$  immobilised in a Nafion film on a glassy carbon electrode, in 30 mM phosphate buffer pH ~7, showing the current enhancement from MWCNT addition. Reproduced from reference<sup>1</sup> with permission from the Royal Society of Chemistry.

Subsequent studies have reported more advanced approaches to immobilize Mn carbonyl catalysts with several achieving notably higher current densities. Reisner and colleagues developed a derivative where the catalyst was anchored to carbon nanotubes through a pyrene-modified bipyridine ligand which was found to show a stable current density of  $0.5 \text{ mA cm}^{-2}$  ( $-1.1 \text{ V}_{\text{SHE}}$ ) with a good selectivity for CO production (maximum Faradic efficiency of 34%) at pH 7.4.<sup>28</sup> Interestingly this system also produced appreciable concentrations of formate, which is not a common observation in other electrocatalytic studies in water described below. Excellent selectivity's for CO production ( $>80\%$  Faradic efficiency) with a stable current density of  $5 \text{ mA cm}^{-2}$  were reported from a polymerised Mn carbonyl complex on MWCNT in a pH 7 electrolyte when  $\text{K}^+$  ions were present at high concentrations.<sup>31</sup> Of great relevance is also the work of Vizza and co-workers who prepared  $[\text{Mn}(\text{apbpy})(\text{CO})_3\text{Br}]$  (apbpy = 4-(4-aminophenyl)-2,2'-bipyridine) which can be electrochemically grafted onto carbon cloth.<sup>32</sup> In this way electrodes with the catalytic centre covalently bound onto the support can be prepared which achieved Faradic efficiencies of ~60% for CO production at  $-1.4 \text{ V}_{\text{Ag}/\text{AgCl}}$  in  $\text{CO}_2$  saturated  $\text{KHCO}_3$ . Very recently studies of this catalyst bound onto a gas diffusion electrode showed that the mass normalised turnover frequencies of the catalyst exceeded those of a benchmark Au catalyst.<sup>33</sup> Another strategy to achieve higher electroactive concentrations of catalytic centres, and therefore potentially higher current densities, is to incorporate the Mn catalytic centre directly within a high surface area porous framework. Examples that use a Mn catalytic centre for  $\text{CO}_2$  reduction in water include as conjugated microporous polymer<sup>34</sup> and a covalent organic framework<sup>35</sup> with the latter achieving an

impressive CO partial current density of  $11 \text{ mA cm}^{-2}$  and selectivity (55% Faradic efficiency) at pH 7.4.<sup>33</sup>

The examples of  $[\text{Mn}(\text{bpy})(\text{CO})_3\text{Br}]$  derivatives immobilised onto, and into, electrode supports for  $\text{CO}_2$  reduction in water have demonstrated that a good level of selectivity (typically  $\geq 1:1 \text{ CO:H}_2$ ) can be achieved at pH  $\sim 7$ . However, it is difficult to quantify the intrinsic selectivity of the catalyst due to the possibility of hydrogen being evolved from the carbon support or impurities within. In order to better understand the behaviour of the Mn catalyst at a wide pH range we also developed a water-soluble Mn diimine  $\text{CO}_2$  reduction complex  $[\text{Mn}(\text{bpy}(\text{COOH})_2)(\text{CO})_3\text{Br}]$ , where  $\text{bpy}(\text{COOH})_2 = 4,4'$ -dicarboxy-2,2'-bipyridine. The solubility of the catalyst allowed for experiments using a Hg amalgam electrode which has a high overpotential for hydrogen evolution making it ideal for analytical electrochemistry in water at a range of pH's.<sup>2</sup> UV/Vis spectroscopy showed a pH dependence due to the changing protonation state of the carboxylate groups, and also indicated that the bromide ligand was readily displaced by water at open circuit. In contrast to the equivalent Re complex<sup>36</sup> where the displacement of the aqua ligand by bicarbonate led to a loss in solubility at some pH's under  $\text{CO}_2$ , the Mn analogue retained solubility under  $\text{CO}_2$  and no evidence of carbonate/bicarbonate ligation was observed.<sup>12</sup> CVs of  $[\text{Mn}^{\text{I}}(\text{bpy}(\text{COO})_2)(\text{CO})_3]^-$  under Ar and  $\text{CO}_2$  at a range of pH's were similar to other complexes from this class in conventional organic solvents with an initial reduction between -1.0 and -1.1  $V_{\text{Ag}/\text{AgCl}}$ , depending upon pH, leading to loss of a solvent ligand and dimer formation and a further reduction between -1.4 and -1.3  $V_{\text{Ag}/\text{AgCl}}$  formed the active  $[\text{Mn}(\text{bpy}(\text{COO})_2)(\text{CO})_3]^{3-}$  (Figure 3a). At the highest pH's studied ( $> 9$ ) minimal  $\text{CO}_2$  reduction occurs, presumably due to a combination of a low concentration of available  $\text{CO}_2$  and  $\text{H}^+$ . Bulk electrolysis was only carried out at a single pH in this initial communication but notably between pH's 9-2.5 a large enhancement in catalytic current occurred under  $\text{CO}_2$  with the greatest increases in current under  $\text{CO}_2$  occurring at the lowest pHs (Figure 3b). This indication of  $\text{CO}_2$  catalysis even at the lowest pH's studied is of particular interest as at pH  $< 4$  bicarbonate formation is no longer a significant process therefore the development and study of catalysts that can operate selectively towards  $\text{CO}_2$  reduction under these conditions may provide a way to enable acid  $\text{CO}_2$  electrolyzers.<sup>26</sup>



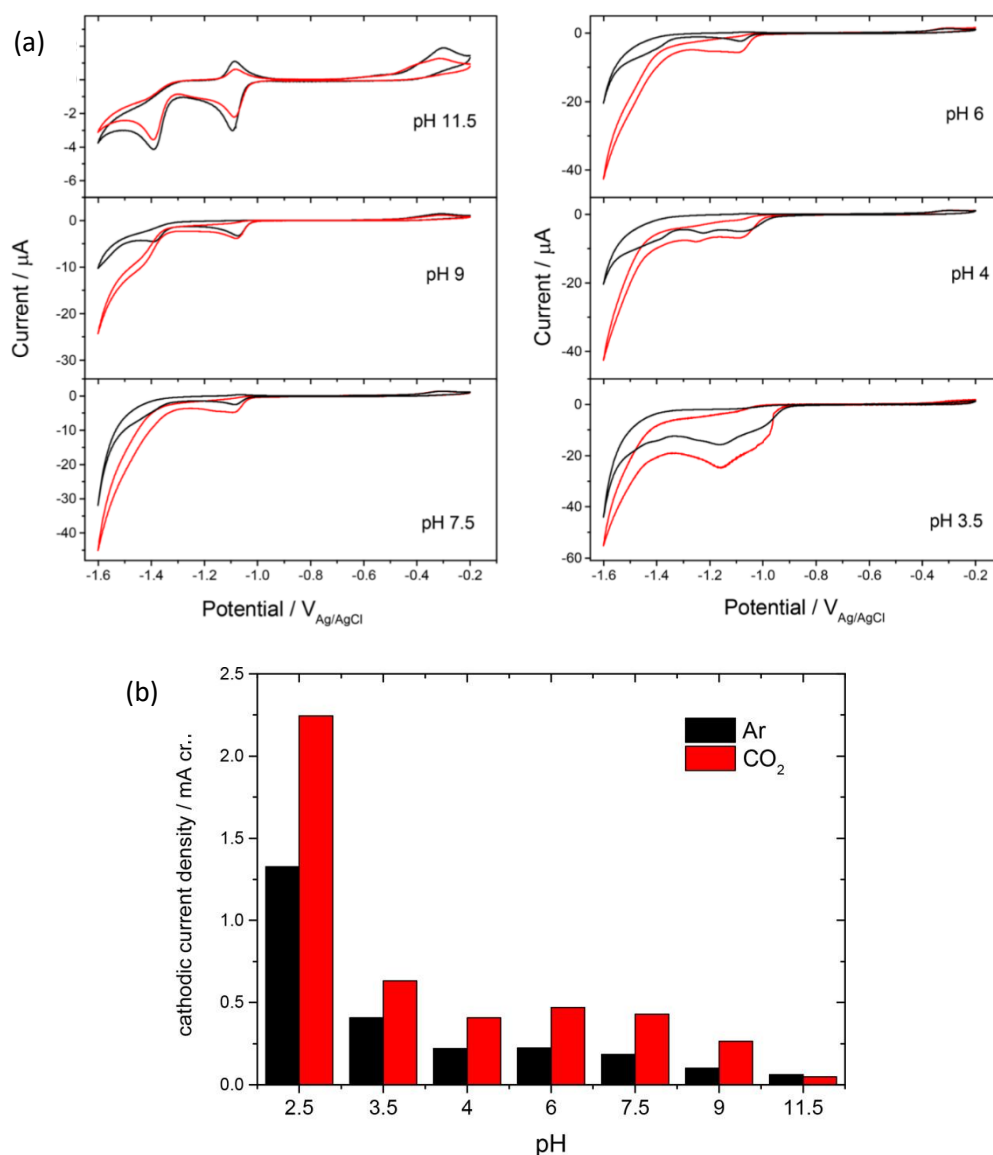


Figure 3.  $[Mn^I(bpy)(COOH)_2(CO)_3Br]$  is a water-soluble  $CO_2$  reduction catalyst that shows good selectivity towards  $CO$  production at pH 9. CV's are shown at a range of pH's under Ar (black) and under  $CO_2$  (red), recorded at  $100\text{ mV s}^{-1}$  (a) Current at  $-1.5\text{ V}_{Ag/AgCl}$  vs. pH under argon (black) and  $CO_2$  (red) (b). Figures reproduced from reference<sup>2</sup> with permission from American Chemical Society.

### 3. Mechanistic studies on $[Mn(bpy)(CO)_3Br]$ at electrode surfaces: understanding the role of the Brønsted acid to rationalise the selectivity towards $CO_2$

The electrochemical behaviour of  $[Mn(bpy)(CO)_3Br]$  has been studied in detail using a wide range of spectroscopic techniques. Covering these in detail is not the aim of this Account and a more comprehensive review is provided by Grills et al.<sup>22</sup> Instead we focus on attempts to understand how these Mn catalysts retain selectivity for  $CO_2$  reduction to  $CO$  in protic environments. As noted in Section 1, two key studies were the original work of Deronzier and colleagues who noted the need for an acid source for catalysis to occur,<sup>20</sup> and work from the Kubiak group on the behaviour of

[Mn(bpy(<sup>t</sup>Bu)<sub>2</sub>)(CO)<sub>3</sub>Br] with a range of acids.<sup>25</sup> In Kubiak's 2013 study it was proposed that the Brønsted acid was required to protonate the initially formed CO<sub>2</sub> adduct, with protonation either stabilizing the Mn-CO<sub>2</sub> species or facilitating the cleavage of a C-O bond. DFT calculations following on from this work by Carter and colleagues confirmed that without an acid present CO<sub>2</sub> binding was endergonic.<sup>37, 38</sup> But once phenol was added the process became exergonic, and initial CO<sub>2</sub> binding was followed by the barrier-less, strongly exergonic protonation of the Mn-CO<sub>2</sub> adduct.<sup>37, 38</sup> This finding has since been further validated and expanded upon in DFT calculations where TFE is the acid source, which showed a dual role for the acid, stabilizing the M-CO<sub>2</sub> adduct with subsequent rapid protonation and exergonic carbonation of the conjugate base providing additional driving force for the overall generation of a Mn-CO<sub>2</sub>H intermediate.<sup>39</sup> The DFT studies of the Carter group also represented the first report of the presence of two catalytic pathways for CO evolution following proton assisted CO<sub>2</sub> binding to [Mn(bpy)(CO)<sub>3</sub>]<sup>-</sup>, labelled the "protonation first" and "reduction first" pathways in Figure 1b. These calculations provided a rationale for the excellent selectivity and improved turnover frequency in the presence of stronger acids, and a framework by which we can understand the selectivity of the catalysts in water. However, direct detection of many of the short-lived intermediates proposed has historically been a challenge with conventional spectroscopies where the need to electrochemically generate high concentrations of species in the bulk inevitably makes the detection of short-lived transient species at the electrode surface difficult.

Our own contribution has focused on using vibrational sum frequency generation (VSFG) spectroscopy to study Mn catalysts at the electrode surface in the presence of a range of acids, with the aim of validating the calculated role of the Brønsted acid in CO<sub>2</sub> reduction. In a VSFG experiment two incident, short laser pulses, are overlapped on the sample of interface (in this case the working electrode surface) and the light is generated at the sum of the frequency of the two input pulses (Figure 4a, b). In our experiments we use a broad-band (typically 500 cm<sup>-1</sup> FWHM, 50 fs) tuneable mid-infrared (mIR) laser and a fixed wavelength visible (800 nm) laser that has a picosecond pulse duration and a time asymmetric shape. Both of these are transmitted through a thin-layer of electrolyte to the electrode surface (Figure 4c and d, for full details of the experimental apparatus see reference<sup>40</sup>). When the mIR laser frequency is resonant with a sum-frequency active vibrational mode the VSFG light intensity is significantly increased and a vibrational spectrum of the species can be recorded. VSFG is often described as surface selective as signals are only generated in a non-centrosymmetric environment under the electric dipole approximation.<sup>41, 42</sup> However it is important to note that across the electrical double layer structure ordering can occur giving rise to VSFG signals and contributions from third order non-linear polarization terms can also arise from molecules throughout the double layer, therefore this statement is not strictly correct.<sup>43, 44</sup> Nonetheless VSFG spectroscopy provides a powerful way to study molecular electrocatalysts whilst they are near (within the double layer structure) or at the electrode surface, as sufficient ordering can occur due to the large electric fields present and the use of catalysts

with non-zero dipole moments. A detailed review on the application of the technique to molecular electrocatalysts is available which describes in more detail the experimental considerations and the route by which spectra are assigned/fitted.<sup>41</sup>

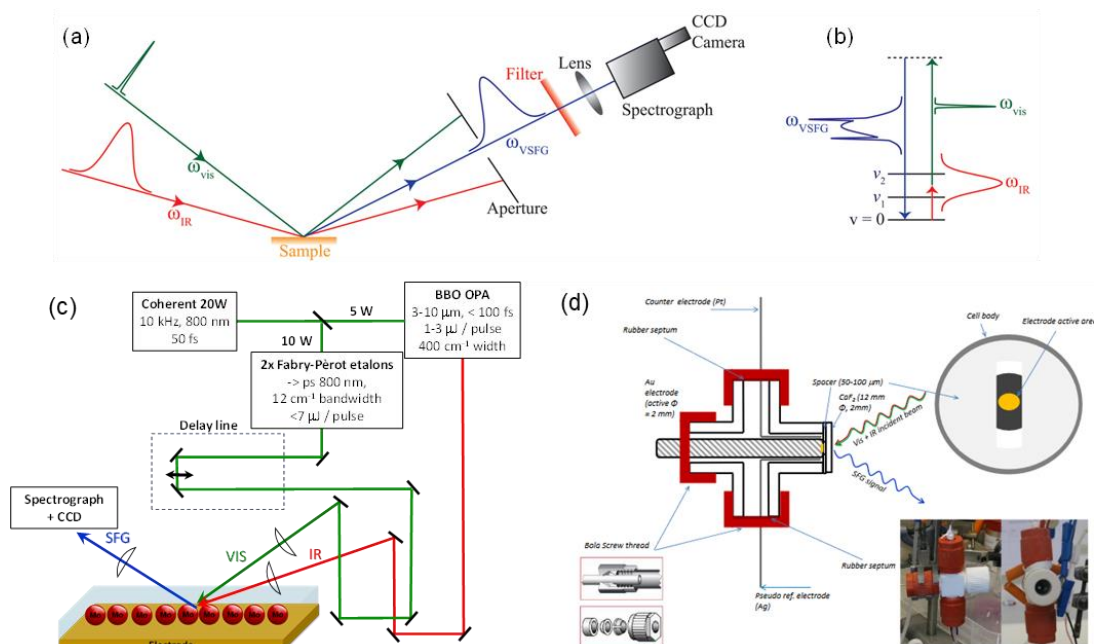


Figure 4 – (a,b) broad-band (<150 fs) mIR VSFG experiments. The data shown here uses a broad-band set-up where a broad band mIR pulse is incident on the electrode surface and overlapped with a narrow-band (> 1 ps) visible laser pulse. (c) Experimental set-up used in the VSFG data in references<sup>3, 4, 40</sup> at the UK Central Laser Facility and (d) SEC cell for VSFG with thin path-length. Figure 4(a,b) reproduced from reference<sup>41</sup> with permission from the PCCP Owner Societies. Figure 4(d) reproduced from reference<sup>40</sup> with permission from American Chemical Society.

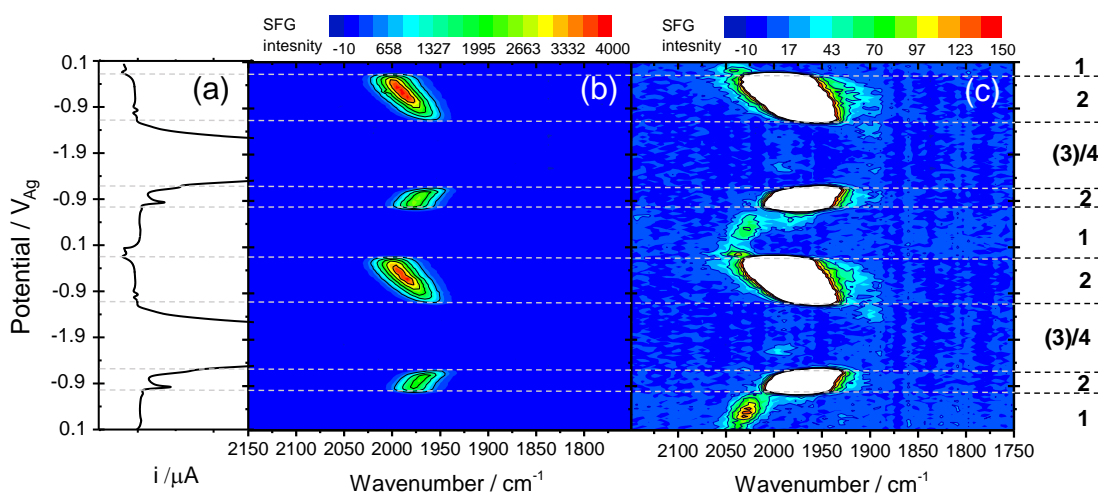


Figure 5. CV (a) of  $[Mn(bpy)(CO)_3Br]$  in  $CH_3CN$  in the presence of 1.5 M TFE under Ar and VSFG spectra (b,c) recorded in-situ of the complex at the working electrode. (c) is an expansion (z-axis, VSFG

intensity) of (b). The numbers on the right correspond to the spectral assignments. 1 =  $[\text{Mn}(\text{bpy})(\text{CO})_3(\text{solv})]^+$ , 2 =  $[\text{Mn}_2\text{bpy}_2(\text{CO})_6]$ , 4 =  $[\text{Mn}(\text{bpy})(\text{CO})_3\text{H}]$ . Figure adapted from reference<sup>3</sup> with permission from Springer Nature.

Initially we have carried out experiments in acetonitrile with added Brønsted acids as the need for IR transmission through the electrolyte prevents the study of aqueous electrolytes. VSFG data recorded during a CV of  $[\text{Mn}(\text{bpy})(\text{CO})_3\text{Br}]$  in  $\text{CH}_3\text{CN}$  with TFE using a static Hg/Au amalgam electrode under an Ar atmosphere is shown in Figure 5.<sup>3</sup> In the VSFG experiments we focus on the metal carbonyl stretching modes as they act as excellent reporter groups on the state of the metal centre and prior bulk SEC-FTIR studies<sup>1, 45-47</sup> provide a way to assign known species at the electrode surface. At open circuit no  $\nu(\text{CO})$  bands were observed, but as the potential of the electrode was swept reductively from +0.1 V to -0.4 V (all potentials in the VSFG experiments in this section are versus a Ag pseudoreference electrode), a strong ( $\sim 2043 \text{ cm}^{-1}$ )  $\nu(\text{CO})$  band increased in intensity (Figure 5c). A 2<sup>nd</sup> broad, much weaker band around  $\sim 1960\text{-}1940 \text{ cm}^{-1}$  could also be observed upon careful inspection of individual spectra (not shown here) with both bands assigned to  $[\text{Mn}(\text{bpy})(\text{CO})_3(\text{CH}_3\text{CN})]^+$  (the solvent can displace the bromide ligand). The  $\nu(\text{CO})$  bands shifted in frequency with applied potential, giving a Stark shift of  $\sim 35 \text{ cm}^{-1} \text{ V}^{-1}$ , demonstrating that the vibrational spectra were occurring from  $[\text{Mn}(\text{bpy})(\text{CO})_3(\text{CH}_3\text{CN})]^+$  experiencing a large electric field which therefore must be at, or near the electrode surface.

As expected from the past FTIR reports,<sup>25, 48</sup> the reduction of  $[\text{Mn}(\text{bpy})(\text{CO})_3(\text{CH}_3\text{CN})]^+$  leads to formation of  $[\text{Mn}_2(\text{bpy})_2(\text{CO})_6]$  (species 2 Figure 1b) and this in turn could be reduced at potentials negative of  $-0.9 \text{ V}_{\text{Ag}}$ . The ISFG of the  $\sim 1970 \text{ cm}^{-1}$  resonant mode of  $[\text{Mn}_2(\text{bpy})_2(\text{CO})_6]$  is very intense (Figure 5B) as the visible laser pulse is resonant with an electronic transition of this complex.<sup>20</sup> We were unable to observe the anticipated active catalyst  $[\text{Mn}(\text{bpy})(\text{CO})_3]^-$  at the electrode surface. Instead,  $[\text{Mn}(\text{bpy})(\text{CO})_3\text{H}]$  formed rapidly (Figure 5) in the absence of  $\text{CO}_2$ . Using VSFG spectroscopy we found in both the absence of a deliberately added, and presence of a number of acids (methanol, TFE, phenol), at the electrode surface we observed  $[\text{Mn}(\text{bpy})(\text{CO})_3\text{H}]$  formation in the absence of  $\text{CO}_2$ .<sup>3, 49</sup> It is clear that at the electrode surface  $[\text{Mn}(\text{bpy})(\text{CO})_3\text{H}]$  formation occurs very rapidly even in the absence of a deliberately added Brønsted acid (trace water is likely present), and the cause of the high selectivity of this complex towards  $\text{CO}_2$  is not the lack of hydride formation. This is an interesting observation as FTIR spectroelectrochemistry had monitored the formation of,  $[\text{Mn}(6,6'\text{-dimesityl-}2,2'\text{-bipyridine})(\text{CO})_3]^-$  in the bulk electrolyte indicating its stability.<sup>50</sup> and DFT calculations<sup>38, 39</sup> predicted a  $\sim 13\text{-}15 \text{ kcal mol}^{-1}$  barrier to binding of  $\text{H}^+$  to  $[\text{Mn}(\text{bpy})(\text{CO})_3]^-$ . One possible rationale of the VSFG result may be the presence of the large electric field at the electrode interface which can have a profound

effect on the relative stability of the species,<sup>51</sup> or due to preferential orientation/accumulation of protons as the electrode surface, with both situations highlighting the need to monitor the surface species.

Under CO<sub>2</sub> with TFE present, in the potential region where CO<sub>2</sub> reduction onsets, [Mn(bpy)(CO)<sub>3</sub>H] is not detected, instead several new  $\nu(\text{CO})$  bands due to CO<sub>2</sub> reduction intermediates appear, Figure 6.<sup>3</sup> The intensity of the VSFG bands of the CO<sub>2</sub> reduction intermediates was greatest with acids with low pK<sub>a</sub>'s. Under CO<sub>2</sub> with the weakest acid studied (e.g. methanol), and when no acid was present, VSFG spectra showed only [Mn(bpy)(CO)<sub>3</sub>H] formation, confirming past predictions that CO<sub>2</sub> binding to [Mn(bpy)(CO)<sub>3</sub>]<sup>-</sup> is endergonic in the absence of a suitably strong acid.<sup>39</sup> Instead in weak acids catalysis is thought to occur *via* the formation of [Mn(bpy)(CO)<sub>3</sub>(CO<sub>2</sub>)<sup>2-</sup> which occurs only at potentials more negative than examined in our work.<sup>39</sup>

Past DFT and microkinetic simulations predicted that [Mn(bpy)(OCOH)] and [Mn(bpy(CO<sub>2</sub>H)]<sup>-</sup> would be the main intermediates observed under CO<sub>2</sub> when TFE and phenol were the acid source at -1.7 and -2.0 V<sub>SCE</sub>, respectively.<sup>37</sup> However, isotopic labelling experiments and DFT calculations of the Stark tuning rates of the  $\nu(\text{CO})$  modes of the CO<sub>2</sub> intermediate ruled out assignment to [Mn(bpy)(OCOH)] and the VSFG bands at ~1976 and 1600 cm<sup>-1</sup> were assigned to [Mn(bpy)(CO)<sub>4</sub>]<sup>+</sup>, a later intermediate in the catalytic cycle of the “protonation first” pathway.<sup>3</sup> The VSFG data did support the proposed potential dependent switching between a protonation first and reduction first pathway,<sup>38, 39</sup> with an additional band at ~1875 cm<sup>-1</sup> possibly being due to [Mn(bpy)(CO<sub>2</sub>H)]<sup>-</sup>. The availability of the lower-overpotential protonation first pathway catalysis had also been demonstrated to occur elsewhere in several studies with derivatives of the Mn complex,<sup>52, 53</sup> and its accessibility offers a further reason for the typically lower overpotentials and increased activity for CO<sub>2</sub> reduction using this class of Mn complexes in the presence of stronger acids.<sup>37, 38</sup>

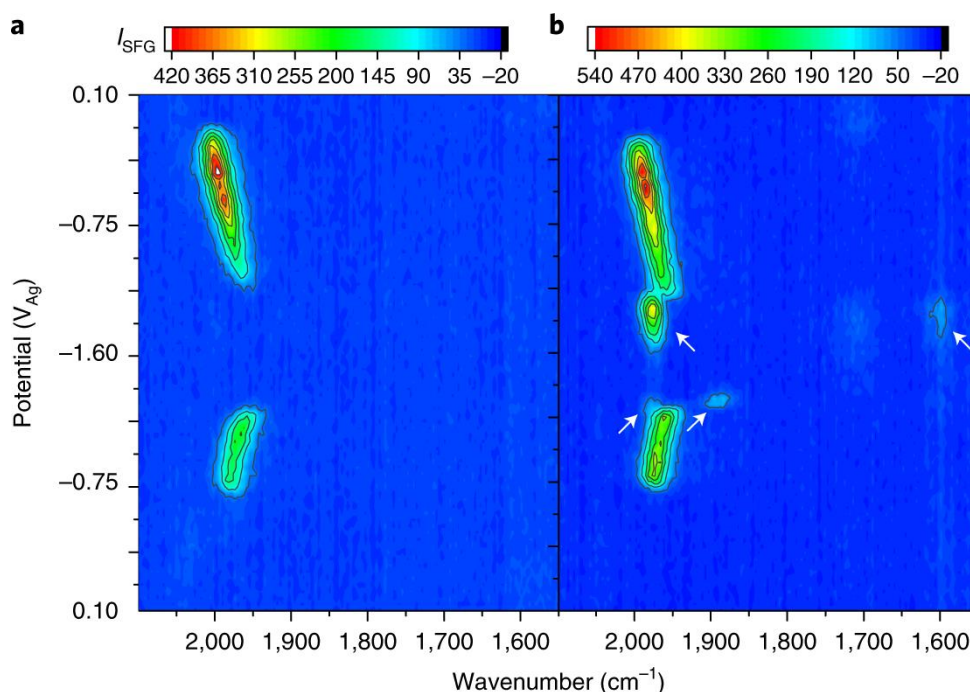


Figure 6. VSFG spectra of  $[\text{Mn}(\text{bpy})(\text{CO})_3\text{Br}]$  in  $\text{CH}_3\text{CN}$  in the presence of 1.5 M TFE under Ar (a) and  $\text{CO}_2$  (b). New  $\text{CO}_2$  reduction intermediates at the electrode surface are indicated with white arrows with the bands at  $\sim 1976$  and  $\sim 1600\text{ cm}^{-1}$  due to  $[\text{Mn}(\text{bpy})(\text{CO})_4]^+$  and a band at  $\sim 1875\text{ cm}^{-1}$  possibly due to  $[\text{Mn}(\text{bpy})(\text{CO}_2\text{H})]$ . Figure reproduced from reference<sup>3</sup> with permission from Springer Nature.

With  $[\text{Mn}(\text{bpy})(\text{CO})_3\text{Br}]$  a  $\text{CO}_2$  reduction current is also observed at potentials positive of  $[\text{Mn}_2(\text{bpy})_2(\text{CO})_6]$  reduction, demonstrating the presence of an additional low-overpotential pathway to produce CO. The catalytic studies outlined in Section 2 show that this “dimer pathway” (Figure 1b) also retains a high selectivity towards CO production even in water. The mechanism of catalysis via the dimer was first studied through a combination of pulsed-EPR and UV/vis spectroscopy<sup>54</sup> where it was shown that in a 5% water/95%  $\text{CH}_3\text{CN}$  solution  $\text{CO}_2$  purging led to loss of electrochemically generated dimer in the bulk electrolyte.<sup>55</sup> Further UV/Vis and FTIR studies of immobilised Mn catalysts also explored the reactivity of the dimer complex in the presence of water and showed it was decreased within seconds of the electrolyte being exposed to  $\text{CO}_2$ .<sup>56, 57</sup> However the behaviour of the dimer using different acid sources had not been previously studied in detail and VSFG spectroscopy also offered a way to analyse the possible role of surface specific species in the “dimer mechanism”.<sup>4</sup>

In a homodyne experiment it can be approximated that VSFG signal intensities scale quadratically with the density of vibrational modes in the interface region.<sup>41</sup> Therefore, a plot of the square root of the VSFG intensities versus electrode potential provides a semiquantitative measure of the surface/double layer concentration of the species. VSFG experiments looking at the behaviour of  $[\text{Mn}_2(\text{bpy})_2(\text{CO})_6]$  in  $\text{CH}_3\text{CN}$  with a range of acids added showed that the dimer accumulated and reached a plateau concentration at  $(-0.7\text{ V}_{\text{Ag}}$ , Figure 7a) in the presence of TFE.<sup>4</sup> Under Ar the surface population of  $[\text{Mn}_2(\text{bpy})_2(\text{CO})_6]$  remained constant regardless of the acid used (TFE, phenol, no acid) until reduction occurred and this led to the formation of  $[\text{Mn}(\text{bpy})(\text{CO})_3\text{H}]$ . Identical behaviour was observed under  $\text{CO}_2$  in the absence of an added acid, with  $[\text{Mn}_2(\text{bpy})_2(\text{CO})_6]$  persisting at the electrode surface prior to  $[\text{Mn}(\text{bpy})(\text{CO})_3\text{H}]$  formation occurring, indicating that  $\text{CO}_2$  is unable to interact with the dimer without a suitable Brønsted acid. In the presence of either TFE or phenol and  $\text{CO}_2$  a notable decrease in the surface concentration of  $[\text{Mn}_2(\text{bpy})_2(\text{CO})_6]$  occurred, 130 mV positive of the reduction potential of  $[\text{Mn}_2(\text{bpy})_2(\text{CO})_6]$ . The extent of decrease in the VSFG signal of  $[\text{Mn}_2(\text{bpy})_2(\text{CO})_6]$  was greatest when the lowest pKa acid (phenol) and  $\text{CO}_2$  were used indicating that  $\text{CO}_2$  interaction with the dimer to produce the previously<sup>54</sup> detected *mer*  $\text{Mn}^{\text{II}}\text{-CO}_2\text{H}$  also occurs *via* a protonation-assisted  $\text{CO}_2$  binding mechanism. Furthermore by analysis of the onset of the catalytic current and from knowledge of the electrochemical stability of previously proposed intermediates a new alternative pathway for CO evolution following *mer*- $\text{Mn}^{\text{II}}\text{-CO}_2\text{H}$  formation *via* the reduction of a *mer*- $\text{Mn}(\text{bpy})(\text{CO})_3(\text{CO}_2\text{H})$  intermediate occurs prior to protonation and  $\text{H}_2\text{O}$  loss (Figure 7b), different to those previously put forward by Deronzier and Grills.<sup>22, 54</sup>

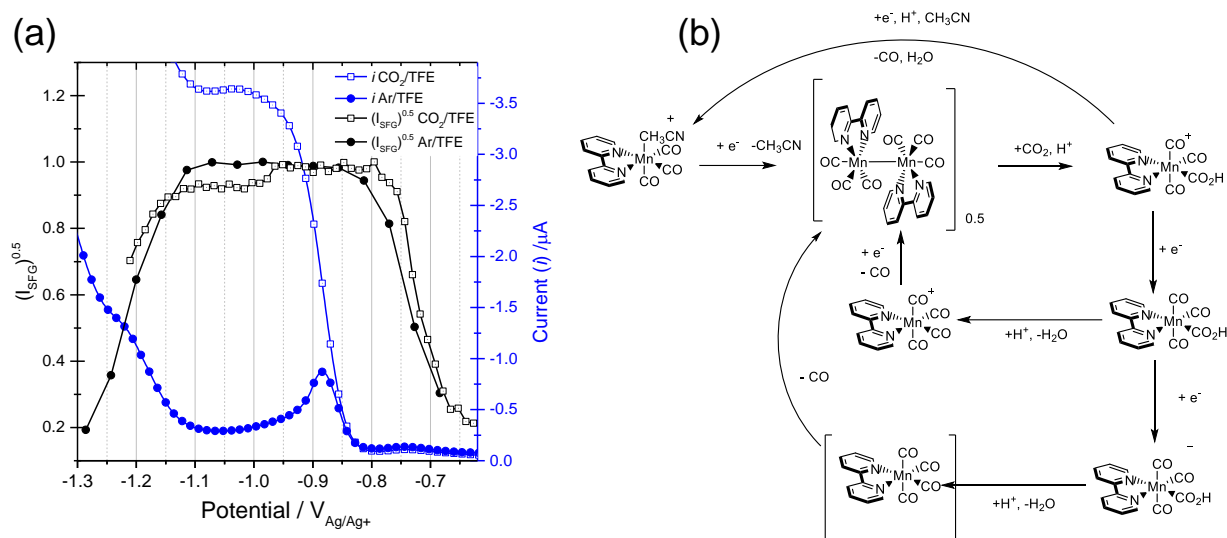


Figure 7. (a) Square root of VSFG intensity of a  $\nu(\text{CO})$  band of  $[\text{Mn}_2(\text{bpy})_2(\text{CO})_6]$  under  $\text{CO}_2$  and Ar gives a measure of the concentration of this species at the electrode as the potential is changed. The current recorded during the experiment is in blue. (b) Analysis of VSFG data leads to a new proposed pathway (bottom) for CO production via the reduction of  $[\text{Mn}(\text{bpy})(\text{CO})_3(\text{CO}_2\text{H})]$ . Reproduced from reference<sup>4</sup> with permission from the PCCP Owner Societies.

## 5. Conclusions and outlook

VSFG spectroscopy can follow the Mn electrocatalyst for  $\text{CO}_2$  reduction whilst at the electrode surface and our results complement the theoretical and other spectroscopic studies in the literature to provide important insights into the remarkable selectivity of this class of catalysts towards  $\text{CO}_2$  reduction. The low levels of  $\text{H}_2$  production are not due to a lack of  $\text{H}^+$  binding when the active  $[\text{Mn}(\text{bpy})(\text{CO})_3]^-$  catalyst is generated as previously postulated, as  $[\text{Mn}(\text{bpy})(\text{CO})_3\text{H}]$  forms rapidly at the electrode surface in the absence of  $\text{CO}_2$ . Instead selectivity towards  $\text{CO}_2$  in all catalytic pathways (“dimer pathway” species: 2, 11; “protonation first”: 3, 5, 6, 8, 9 and “reduction first”: 3, 5, 6, 7, 9, Figure 1B) arises by an unusual acid-promoted  $\text{CO}_2$  binding mechanism, where acids with a lower pKa actually lead to higher concentrations of  $\text{CO}_2$  reduction intermediates. We believe that such an effect has been rarely reported within the large variety of known homogeneous  $\text{CO}_2$  reduction catalysts. To date our studies have focused on one particular class of catalysts, and not in aqueous solvent, which may complicate direct comparisons, but we encourage future works to explore if similar proton-assisted  $\text{CO}_2$  binding mechanisms are in wider operation amongst  $\text{CO}_2$  reduction catalysts.

Recent technoeconomic analyses highlight the need to understand, and discover new, electrocatalysts that can reduce  $\text{CO}_2$  selectively in water, in particular at low pH's.<sup>27</sup> There are relatively

few studies to date on the use of this class of catalysts in water but from the emerging literature it does appear that the proton-assisted CO<sub>2</sub> binding mechanisms seen in aprotic solvents may be facilitating the measured high levels of selectivity in aqueous electrolytes as well. Whilst the long-term stability of these Mn catalysts is uncertain, especially under high current densities, initial catalysis studies are promising and these Mn complexes serve as valuable models for future development of proton/acid tolerant CO<sub>2</sub> reduction catalysts.

## **Acknowledgements**

AC and BS acknowledge UKRI-EPSC (EP/V011863/1) for financial support. CE acknowledges NSG Pilkington for support of the PhD studentship. The authors also wish to thank both present and past colleagues for their contributions to the science described in this account.

## **Biographies**

Bhavin Siritanaratkul received his DPhil in Chemistry from the University of Oxford under the supervision of Fraser A. Armstrong, where he worked on the electrochemistry of enzymes for nicotinamide cofactor regeneration. His prior research experience includes solar water splitting and heterogeneous catalysis for methane conversion. He is currently a postdoctoral researcher with Alex Cowan at the University of Liverpool, working on electrochemical CO<sub>2</sub> reduction.

Catherine Eagle obtained her Masters in Science from Imperial College London (2020) under the supervision of Dr Rob Davies. Following this, she moved to the University of Liverpool to join Prof. Alex Cowan's research group as a PhD student to study carbon dioxide utilisation by selective reduction of impure and low concentration carbon dioxide streams using molecular catalysts.

Alex Cowan is a Professor of Chemistry at the University of Liverpool where he leads an interdisciplinary team who are developing new, and studying the mechanisms of, catalysts and materials for the production of sustainable fuels. A particular interest of the group is the electrocatalytic reduction of carbon dioxide into useful molecules such as carbon monoxide and the in-situ studies of these electrocatalysts.

## **References**



1. Walsh, J. J.; Neri, G.; Smith, C. L.; Cowan, A. J., Electrocatalytic CO<sub>2</sub> reduction with a membrane supported manganese catalyst in aqueous solution. *Chem. Commun.* **2014**, *50* (84), 12698-12701.
2. Walsh, J. J.; Neri, G.; Smith, C. L.; Cowan, A. J., Water-Soluble Manganese Complex for Selective Electrocatalytic CO<sub>2</sub> Reduction to CO. *Organometallics* **2019**, *38* (6), 1224-1229.
3. Neri, G.; Walsh, J. J.; Teobaldi, G.; Donaldson, P. M.; Cowan, A. J., Detection of catalytic intermediates at an electrode surface during carbon dioxide reduction by an earth-abundant catalyst. *Nature Catalysis* **2018**, *1* (12), 952-959.
4. Neri, G.; Donaldson, P. M.; Cowan, A. J., In situ study of the low overpotential "dimer pathway" for electrocatalytic carbon dioxide reduction by manganese carbonyl complexes. *Physical Chemistry Chemical Physics* **2019**, *21* (14), 7389-7397.
5. Kibria, M. G.; Edwards, J. P.; Gabardo, C. M.; Dinh, C.-T.; Seifitokaldani, A.; Sinton, D.; Sargent, E. H., Electrochemical CO<sub>2</sub> Reduction into Chemical Feedstocks: From Mechanistic Electrocatalysis Models to System Design. *Adv. Mater.* **2019**, *31* (31), 1807166.
6. Birdja, Y. Y.; Pérez-Gallent, E.; Figueiredo, M. C.; Göttle, A. J.; Calle-Vallejo, F.; Koper, M. T. M., Advances and challenges in understanding the electrocatalytic conversion of carbon dioxide to fuels. *Nature Energy* **2019**, *4* (9), 732-745.
7. Francke, R.; Schille, B.; Roemelt, M., Homogeneously Catalyzed Electroreduction of Carbon Dioxide-Methods, Mechanisms, and Catalysts. *Chem Rev* **2018**, *118* (9), 4631-4701.
8. Hori, Y., Electrochemical CO<sub>2</sub> Reduction on Metal Electrodes. In *Modern Aspects of Electrochemistry*, Vayenas, C. G.; White, R. E.; Gamboa-Aldeco, M. E., Eds. Springer New York: New York, NY, 2008; pp 89-189.
9. García de Arquer, F. P.; Dinh, C.-T.; Ozden, A.; Wicks, J.; McCallum, C.; Kirmani Ahmad, R.; Nam, D.-H.; Gabardo, C.; Seifitokaldani, A.; Wang, X.; Li Yuguang, C.; Li, F.; Edwards, J.; Richter Lee, J.; Thorpe Steven, J.; Sinton, D.; Sargent Edward, H., CO<sub>2</sub> electrolysis to multicarbon products at activities greater than 1 A cm<sup>-2</sup>. *Science* **2020**, *367* (6478), 661-666.
10. Li, C.; Xiong, H.; He, M.; Xu, B.; Lu, Q., Oxyhydroxide Species Enhances CO<sub>2</sub> Electroreduction to CO on Ag via Coelectrolysis with O<sub>2</sub>. *ACS Catalysis* **2021**, *11* (19), 12029-12037.
11. Xu, Y.; Edwards, J. P.; Zhong, J.; O'Brien, C. P.; Gabardo, C. M.; McCallum, C.; Li, J.; Dinh, C.-T.; Sargent, E. H.; Sinton, D., Oxygen-tolerant electroproduction of C<sub>2</sub> products from simulated flue gas. *Energy & Environmental Science* **2020**, *13* (2), 554-561.
12. Jiang, C.; Nichols, A. W.; Machan, C. W., A look at periodic trends in d-block molecular electrocatalysts for CO<sub>2</sub> reduction. *Dalton Trans* **2019**, *48* (26), 9454-9468.
13. Kinzel, N. W.; Werle, C.; Leitner, W., Transition Metal Complexes as Catalysts for the Electroconversion of CO<sub>2</sub> : An Organometallic Perspective. *Angew. Chem. Int. Ed. Engl.* **2021**, *60* (21), 11628-11686.
14. Liu, D.-C.; Zhong, D.-C.; Lu, T.-B., Non-noble metal-based molecular complexes for CO<sub>2</sub> reduction: From the ligand design perspective. *EnergyChem* **2020**, *2* (3), 100034.
15. Amanullah, S.; Saha, P.; Nayek, A.; Ahmed, M. E.; Dey, A., Biochemical and artificial pathways for the reduction of carbon dioxide, nitrite and the competing proton reduction: effect of 2(nd) sphere interactions in catalysis. *Chem. Soc. Rev.* **2021**, *50* (6), 3755-3823.
16. Hawecker, J.; Lehn, J.-M.; Ziessel, R., Electrocatalytic reduction of carbon dioxide mediated by Re(bipy)(CO)<sub>3</sub>Cl (bipy = 2,2'-bipyridine). *J. Chem. Soc., Chem. Commun.* **1984**, (6), 328-330.
17. Hawecker, J.; Lehn, J.-M.; Ziessel, R., Efficient photochemical reduction of CO<sub>2</sub> to CO by visible light irradiation of systems containing Re(bipy)(CO)<sub>3</sub>X or Ru(bipy)<sub>3</sub><sup>2+</sup>-Co<sup>2+</sup> combinations as homogeneous catalysts. *J. Chem. Soc., Chem. Commun.* **1983**, (9), 536-538.
18. Yaroshevsky, A. A., Abundances of chemical elements in the Earth's crust. *Geochemistry International* **2006**, *44* (1), 48-55.
19. Johnson, F. P. A.; George, M. W.; Hartl, F.; Turner, J. J., Electrocatalytic Reduction of CO<sub>2</sub> Using the Complexes [Re(bpy)(CO)<sub>3</sub>L]<sub>n</sub> (n = +1, L = P(OEt)<sub>3</sub>, CH<sub>3</sub>CN; n = 0, L = Cl<sup>-</sup>, Otf<sup>-</sup>; bpy = 2,2'-

Bipyridine; Otf- = CF<sub>3</sub>SO<sub>3</sub>) as Catalyst Precursors: Infrared Spectroelectrochemical Investigation. *Organometallics* **1996**, *15* (15), 3374-3387.

20. Bourrez, M.; Molton, F.; Chardon-Noblat, S.; Deronzier, A., [Mn(bipyridyl)(CO)<sub>3</sub>Br]: an abundant metal carbonyl complex as efficient electrocatalyst for CO<sub>2</sub> reduction. *Angew. Chem. Int. Ed. Engl.* **2011**, *50* (42), 9903-6.
21. Barrett, J. A.; Miller, C. J.; Kubiak, C. P., Electrochemical Reduction of CO<sub>2</sub> Using Group VII Metal Catalysts. *Trends in Chemistry* **2021**, *3* (3), 176-187.
22. Grills, D. C.; Ertem, M. Z.; McKinnon, M.; Ngo, K. T.; Rochford, J., Mechanistic aspects of CO<sub>2</sub> reduction catalysis with manganese-based molecular catalysts. *Coord. Chem. Rev.* **2018**, *374*, 173-217.
23. Sinopoli, A.; La Porte, N. T.; Martinez, J. F.; Wasielewski, M. R.; Sohail, M., Manganese carbonyl complexes for CO<sub>2</sub> reduction. *Coord. Chem. Rev.* **2018**, *365*, 60-74.
24. Stanbury, M.; Compain, J.-D.; Chardon-Noblat, S., Electro and photoreduction of CO<sub>2</sub> driven by manganese-carbonyl molecular catalysts. *Coord. Chem. Rev.* **2018**, *361*, 120-137.
25. Smieja, J. M.; Sampson, M. D.; Grice, K. A.; Benson, E. E.; Froehlich, J. D.; Kubiak, C. P., Manganese as a Substitute for Rhenium in CO<sub>2</sub> Reduction Catalysts: The Importance of Acids. *Inorg. Chem.* **2013**, *52* (5), 2484-2491.
26. Li, J.; Kornienko, N., Electrocatalytic carbon dioxide reduction in acid. *Chem Catalysis* **2022**, *2* (1), 29-38.
27. Rabinowitz, J. A.; Kanan, M. W., The future of low-temperature carbon dioxide electrolysis depends on solving one basic problem. *Nature Communications* **2020**, *11* (1), 5231.
28. Reuillard, B.; Ly, K. H.; Rosser, T. E.; Kuehnel, M. F.; Zebger, I.; Reisner, E., Tuning Product Selectivity for Aqueous CO<sub>2</sub> Reduction with a Mn(bipyridine)-pyrene Catalyst Immobilized on a Carbon Nanotube Electrode. *J. Am. Chem. Soc.* **2017**, *139* (41), 14425-14435.
29. Yoshida, T.; Tsutsumida, K.; Teratani, S.; Yasufuku, K.; Kaneko, M., Electrocatalytic reduction of CO<sub>2</sub> in water by [Re(bpy)(CO)<sub>3</sub>Br] and [Re(terpy)(CO)<sub>3</sub>Br] complexes incorporated into coated nafion membrane (bpy = 2,2'-bipyridine; terpy = 2,2';6',2''-terpyridine). *J. Chem. Soc., Chem. Commun.* **1993**, (7), 631-633.
30. Walsh, J. J.; Smith, C. L.; Neri, G.; Whitehead, G. F. S.; Robertson, C. M.; Cowan, A. J., Improving the efficiency of electrochemical CO<sub>2</sub> reduction using immobilized manganese complexes. *Faraday Discuss.* **2015**, *183* (0), 147-160.
31. Sato, S.; Saita, K.; Sekizawa, K.; Maeda, S.; Morikawa, T., Low-Energy Electrocatalytic CO<sub>2</sub> Reduction in Water over Mn-Complex Catalyst Electrode Aided by a Nanocarbon Support and K<sup>+</sup> Cations. *ACS Catalysis* **2018**, *8* (5), 4452-4458.
32. Rotundo, L.; Filippi, J.; Gobetto, R.; Miller, H. A.; Rocca, R.; Nervi, C.; Vizza, F., Electrochemical CO<sub>2</sub> reduction in water at carbon cloth electrodes functionalized with a fac-Mn(apbpy)(CO)<sub>3</sub>Br complex. *Chem. Commun.* **2019**, *55* (6), 775-777.
33. Filippi, J.; Rotundo, L.; Gobetto, R.; Miller, H. A.; Nervi, C.; Lavacchi, A.; Vizza, F., Turning manganese into gold: Efficient electrochemical CO<sub>2</sub> reduction by a fac-Mn(apbpy)(CO)<sub>3</sub>Br complex in a gas-liquid interface flow cell. *Chem. Eng. J.* **2021**, *416*, 129050.
34. Smith, C. L.; Clowes, R.; Sprick, R. S.; Cooper, A. I.; Cowan, A. J., Metal-organic conjugated microporous polymer containing a carbon dioxide reduction electrocatalyst. *Sustainable Energy & Fuels* **2019**, *3* (11), 2990-2994.
35. Dubed Bandomo, G. C.; Mondal, S. S.; Franco, F.; Bucci, A.; Martin-Diaconescu, V.; Ortuño, M. A.; van Langevelde, P. H.; Shafir, A.; López, N.; Lloret-Fillol, J., Mechanically Constrained Catalytic Mn(CO)<sub>3</sub>Br Single Sites in a Two-Dimensional Covalent Organic Framework for CO<sub>2</sub> Electroreduction in H<sub>2</sub>O. *ACS Catalysis* **2021**, *11* (12), 7210-7222.
36. Nakada, A.; Ishitani, O., Selective Electrocatalysis of a Water-Soluble Rhenium(I) Complex for CO<sub>2</sub> Reduction Using Water As an Electron Donor. *ACS Catalysis* **2018**, *8* (1), 354-363.
37. Riplinger, C.; Carter, E. A., Influence of Weak Brønsted Acids on Electrocatalytic CO<sub>2</sub> Reduction by Manganese and Rhenium Bipyridine Catalysts. *ACS Catalysis* **2015**, *5* (2), 900-908.

38. Riplinger, C.; Sampson, M. D.; Ritzmann, A. M.; Kubiak, C. P.; Carter, E. A., Mechanistic contrasts between manganese and rhenium bipyridine electrocatalysts for the reduction of carbon dioxide. *J. Am. Chem. Soc.* **2014**, *136* (46), 16285-98.
39. Lam, Y. C.; Nielsen, R. J.; Gray, H. B.; Goddard, W. A., A Mn Bipyrimidine Catalyst Predicted To Reduce CO<sub>2</sub> at Lower Overpotential. *ACS Catalysis* **2015**, *5* (4), 2521-2528.
40. Neri, G.; Donaldson, P. M.; Cowan, A. J., The Role of Electrode–Catalyst Interactions in Enabling Efficient CO<sub>2</sub> Reduction with Mo(bpy)(CO)<sub>4</sub> As Revealed by Vibrational Sum-Frequency Generation Spectroscopy. *Journal of the American Chemical Society* **2017**, *139* (39), 13791-13797.
41. Gardner, A. M.; Saeed, K. H.; Cowan, A. J., Vibrational sum-frequency generation spectroscopy of electrode surfaces: studying the mechanisms of sustainable fuel generation and utilisation. *Phys. Chem. Chem. Phys.* **2019**, *21* (23), 12067-12086.
42. Lambert, A. G.; Davies, P. B.; Neivandt, D. J., Implementing the Theory of Sum Frequency Generation Vibrational Spectroscopy: A Tutorial Review. *Applied Spectroscopy Reviews* **2005**, *40* (2), 103-145.
43. Rey, N. G.; Dlott, D. D., Studies of electrochemical interfaces by broadband sum frequency generation. *J. Electroanal. Chem.* **2017**, *800*, 114-125.
44. Ohno, P. E.; Wang, H.-f.; Geiger, F. M., Second-order spectral lineshapes from charged interfaces. *Nature Communications* **2017**, *8* (1), 1032.
45. Grills, D. C.; Farrington, J. A.; Layne, B. H.; Lymar, S. V.; Mello, B. A.; Preses, J. M.; Wishart, J. F., Mechanism of the formation of a Mn-based CO<sub>2</sub> reduction catalyst revealed by pulse radiolysis with time-resolved infrared detection. *J. Am. Chem. Soc.* **2014**, *136* (15), 5563-6.
46. Franco, F.; Cometto, C.; Nencini, L.; Barolo, C.; Sordello, F.; Minero, C.; Fiedler, J.; Robert, M.; Gobetto, R.; Nervi, C., Local Proton Source in Electrocatalytic CO<sub>2</sub> Reduction with [Mn(bpy-R)(CO)<sub>3</sub> Br] Complexes. *Chemistry* **2017**, *23* (20), 4782-4793.
47. Scheiring, T.; Kaim, W.; Fiedler, J., Geometrical and electronic structures of the acetyl complex Re(bpy)(CO)<sub>3</sub>(COCH<sub>3</sub>) and of [M(bpy)(CO)<sub>4</sub>](OTf), M=Mn,Re. *J. Organomet. Chem.* **2000**, *598* (1), 136-141.
48. Machan, C. W.; Sampson, M. D.; Chabolla, S. A.; Dang, T.; Kubiak, C. P., Developing a Mechanistic Understanding of Molecular Electrocatalysts for CO<sub>2</sub> Reduction using Infrared Spectroelectrochemistry. *Organometallics* **2014**, *33* (18), 4550-4559.
49. Neri, G.; Donaldson, P. M.; Cowan, A. J. *Vibrational Sum Frequency Generation (VSFG) Spectroscopy of Electrocatalytic Mechanisms*; CLF Annual Report, 2017.
50. Sampson, M. D.; Nguyen, A. D.; Grice, K. A.; Moore, C. E.; Rheingold, A. L.; Kubiak, C. P., Manganese Catalysts with Bulky Bipyridine Ligands for the Electrocatalytic Reduction of Carbon Dioxide: Eliminating Dimerization and Altering Catalysis. *Journal of the American Chemical Society* **2014**, *136* (14), 5460-5471.
51. Schultz, Z. D.; Shaw, S. K.; Gewirth, A. A., Potential Dependent Organization of Water at the Electrified Metal–Liquid Interface. *Journal of the American Chemical Society* **2005**, *127* (45), 15916-15922.
52. Ngo, K. T.; McKinnon, M.; Mahanti, B.; Narayanan, R.; Grills, D. C.; Ertem, M. Z.; Rochford, J., Turning on the Protonation-First Pathway for Electrocatalytic CO<sub>2</sub> Reduction by Manganese Bipyridyl Tricarbonyl Complexes. *Journal of the American Chemical Society* **2017**, *139* (7), 2604-2618.
53. Yang, Y.; Ertem, M. Z.; Duan, L., An amide-based second coordination sphere promotes the dimer pathway of Mn-catalyzed CO<sub>2</sub>-to-CO reduction at low overpotential. *Chemical Science* **2021**, *12* (13), 4779-4788.
54. Bourrez, M.; Orio, M.; Molton, F.; Vezin, H.; Duboc, C.; Deronzier, A.; Chardon-Noblat, S., Pulsed-EPR evidence of a manganese(II) hydroxycarbonyl intermediate in the electrocatalytic reduction of carbon dioxide by a manganese bipyridyl derivative. *Angew. Chem. Int. Ed. Engl.* **2014**, *53* (1), 240-3.
55. Hayashi, Y.; Kita, S.; Brunschwig, B. S.; Fujita, E., Involvement of a Binuclear Species with the Re–C(O)O–Re Moiety in CO<sub>2</sub> Reduction Catalyzed by Tricarbonyl Rhenium(I) Complexes with Diimine

Ligands: Strikingly Slow Formation of the Re–Re and Re–C(O)O–Re Species from Re(dmb)(CO)3S (dmb = 4,4'-Dimethyl-2,2'-bipyridine, S = Solvent). *Journal of the American Chemical Society* **2003**, *125* (39), 11976-11987.

56. Rosser, T. E.; Windle, C. D.; Reisner, E., Electrocatalytic and Solar-Driven CO<sub>2</sub> Reduction to CO with a Molecular Manganese Catalyst Immobilized on Mesoporous TiO<sub>2</sub>. *Angew. Chem. Int. Ed. Engl.* **2016**, *55* (26), 7388-92.

57. Walsh, J. J.; Forster, M.; Smith, C. L.; Neri, G.; Potter, R. J.; Cowan, A. J., Directing the mechanism of CO<sub>2</sub> reduction by a Mn catalyst through surface immobilization. *Physical Chemistry Chemical Physics* **2018**, *20* (10), 6811-6816.